Wave Power Enhancement Caused by a dc Electric Field

By Osamu FUKUMASA* and Setsuo SAEKI*

(Received July 15, 1985)

Abstract

The effect of a dc electric field on the spatial evolution of the two stream instability in a small cold beam–plasma system is investigated by using a model of many waves. The wave enhancement is dependent on the growth of neighboring waves. Weak collisions also play an important role in limiting the wave enhancement.

1. Introduction

When a small and fast monoenergetic electron beam passes through a plasma, the combined system is unstable to the growth of waves. The unstable waves have phase velocities slightly slower than the beam drift velocity v_b and extract energy from the beam by slowing down the beam electrons on the average. When the beam has slowed to the average wave phase velocity, the instability saturates and the beam becomes electrostatically trapped in the wave trough.[1-3)]

Recently, it has been predicted that the application of an external dc electric field E_{dc} to particles trapped in the potential well of a wave can result in an increase in wave amplitude.[4)] This effect has been observed experimentally in a traveling wave tube (TWT).[5)] On the practical side, saturation by beam trapping limits the maximum energy that can be extracted in a TWT. Therefore, control of the trapped beam offers the possibility of enhancing the efficiency of energy extraction out of beam devices. Moreover, the energy exchange process in a free electron laser (FEL) is quite similar to that of a TWT. In the FEL the application of E_{dc} to trapped beam electrons has been proposed as a possible wave power enhancement scheme by Lin.[6)]

As the equations that describe the wave–particle interaction in a TWT are identical to those that describe the beam–plasma instability in the small cold beam limit, the modification of the dynamics of beam trapping caused by E_{dc} is of interest to basic plasma physics studies. Previously, we confirmed, by means of a single wave model, detuning and collisional effects on wave enhancement caused by E_{dc} in a small cold beam–plasma system.[7,8)]

The single wave model has assumed that in the nonlinear stage the wave electric field spectrum is sharply peaked at the frequency of the most unstable wave and that the entire spectrum is replaced by a single wave.[1,2)] But, under a certain plasma condition, the wave spectrum is very broad and the beam electrons are significantly influenced by many waves. Therefore, by using a model of many waves,[9-11)] we study the wave evolution in the presence of E_{dc} in detail and weak collisional effects on wave enhancement.

*Department of Electrical Engineering

2. Simulation Model

2.1 Basic equations

In this paper, we consider the spatial evolution of a system consisted of many modes. We make simulation by using the model of the eleven modes where five modes are located on each side of the most unstable wave (frequency ω_0). The freguency of each mode is given by $\omega = \omega_0 + n\Delta\omega$, where $n = 0, \pm 1 \cdots \pm 5$, and $\Delta\omega$ is a frequency separation between modes.

The intensity of the wave electric field, E (x, t), with a stationary amplitude E (0) is written as

$$E(x, t) = \sum_{\omega} E_{\omega}(x) \exp(-i\omega t) \quad + \quad \text{c. c.} \quad , \tag{1}$$

where $E_{\omega}(x) = E_{\omega}(0) \exp\left(i\int_0^x k_{\omega}(x')\,dx'\right)$. From Poisson's equation for each Fourier component of the electric field, $E_{\omega}(x)$, and the equation of motion for individual particles of beam electrons, the self–consistent interaction of a beam, a non–resonant plasma and many waves are calculated using a computer.

According to our previous model,[7,11] the following system of equations is obtained in standard notation :

$$\left(A + iB + iC\frac{d}{d\eta} + D\frac{d^2}{d\eta^2}\right) E_{\omega}(\eta) = \frac{i}{N}\sum_j \exp(i\omega\xi_j/\omega_0) , \tag{2}$$

$$\frac{d^2\xi_j}{d\eta^2} = \left(1+s\frac{d\xi_j}{d\eta}\right)^3 \left[\sum_{\omega} E_{\omega}(\eta) \exp(-i\omega\xi_j/\omega_0) + \text{c. c.}\right]$$

$$- \left(1 + s\frac{d\xi_j}{d\eta}\right)^3 E_{dc} , \tag{3}$$

where $A = s^2\frac{\omega_0^2}{\omega_b^2}\left[(1 + \delta\omega/\omega_0) - (1 + \delta\omega/\omega_0)^{-1}\right]$,

$$B = s^2\frac{\nu}{\omega_0}\frac{\omega_0^2}{\omega_b^2}(1 + \delta\omega/\omega_0)^{-2},$$

$$C = (1 + \delta\omega/\omega_0)^{-2}, \qquad D = \frac{s}{2}(1 + \delta\omega/\omega_0)^{-3},$$

$$s = \left(\frac{1}{6}\frac{n_b}{n_p}\frac{v_b^2}{v_t^2}\right)^{1/3} \quad \text{and} \quad \omega_0^2 = \omega_p^2(1 + 3v_t^2/v_b^2) .$$

The coefficient A is derived from a detuning effect, i. e. $\delta\omega = \omega - \omega_0$. The coefficient B is dervied from a collisional effect because ν is the effective collision frequency between plasma electrons.[12] The quantity s is the spatial scaling factor. We also call s beam strength[9] because the half–width of the growth rate function is proportional to s. The normalized electric field of the wave $E_{\omega}(\eta)$ and the spatial coordinate η are de-

fined by $E_\omega(\eta) = eE_\omega(x) \exp(-ix\omega/v_b)/(mv_b\omega_0 s^2)$ and $\eta = sx(\omega_0/v_b)$, respectively. Here, E_{dc} is also the normalized dc electric field. The phase-space coordinate of the j-th beam electron ξ_j is defined as $\xi_j = \omega_0[t_j(x) - x/v_b]$. The function $t_j(x)$ is the time when the j-th beam passes the point x. The velocity $v_j = \dot{x}_j$ in the laboratory frame is obtained from $\dot{\xi}_j = d\xi_j/d\eta$ by using the relation $\dot{x}_j = v_b/(1+s\dot{\xi}_j)$.

2.2 Method of numerical calculation

In order to solve equations (2) and (3), we represent the beams by N charge sheets and solve for the exact nonlinear dynamics numerically. The equations are integrated with the Runge-Kutta method with a step size of $\Delta\eta = 0.05$. The initial wave amplitudes are equal to 10^{-3}.

The initial conditions required for beam particles are as follows: For many wave system, we need to follow the beam particles whose initial phases are in the interval $0 \leq \xi_j(0) \leq 2\pi l$ to satisfy the periodic boundary conditions, where l is an integer and $l = \omega_0/\Delta\omega$. Therefore, initial conditions are

$$\xi_j(0) = 2\pi l(j/N) \qquad \text{and} \qquad \dot{\xi}_j(0) = 0. \tag{4}$$

The number of particles in one period is N/l. If we keep N/l constant, a closer mode spacing would require a large number of beam electrons N. When $\Delta\omega/\omega_0 = 0.02$ (i. e. l = 50), 200, 400, 600 and 1000 beam sheets are used. There are no significant differences among last three cases. Here, we show the results for $\Delta\omega/\omega_0 = 0.02$ and N = 600.

3. Numerical Results and Discussion

3.1 Linear dispersion relation in the beam-plasma system

Simulation has been done for two situations, i. e. Case I where the wave spectrum can be replaced by a single wave and Case II where the wave spectrum is broad. In the former case, plasma parameters are chosen as follows: A ratio of beam electron to plasma electron densities $n_b/n_p = 3.1 \times 10^{-4}$ and a ratio of beam velocity to plasma thermal velocity $v_b/v_t = 9$. In the latter case, $n_b/n_p = 10^{-3}$ and $v_b/v_t = 5$.

In a cold beam – a weakly collisional and warm plasma system, a linear dispersion relation is written as follows:

$$\varepsilon(\omega, k) = 1 - \frac{\omega_p^2}{\omega(\omega + i\nu) - 3k^2v_t^2} - \frac{\omega_b^2}{(\omega - kv_b)^2} = 0, \tag{5}$$

where ω_p and ω_b are the electron plasma frequency of the background plasma and that of beam electrons. In order to see the characteristics of the spatially growing waves, dispersion equation (5) must be solved for a complex wavenumber k for a given real frequency ω.

Figures 1 and 2 show the numerical solutions of eq. (5) for the Case I and Case II, respectively. A branch labeled a is a mode of beam space charge wave, and a branch

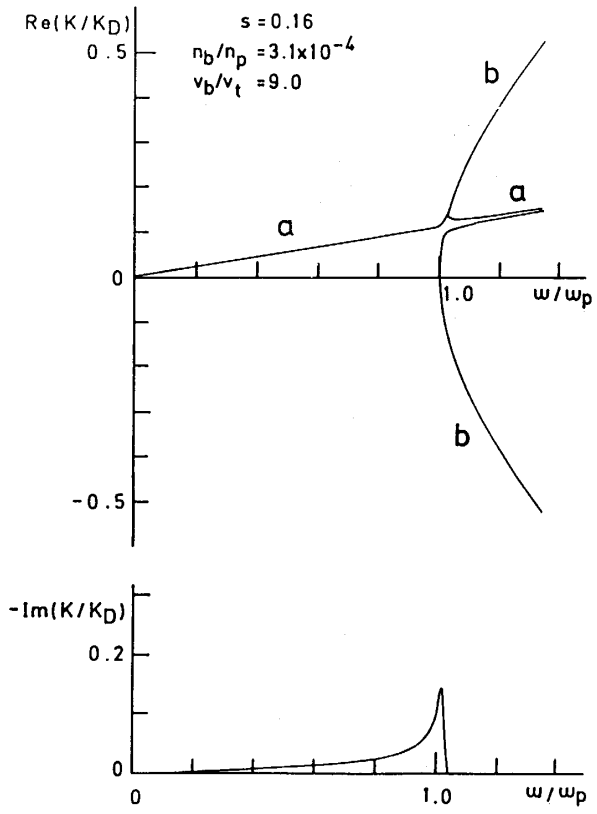

Fig. 1 Numerical solution of the linear dispersion equation in a beam–plasma system (Case I).
Upper : Real part of the wavenumber k/k_D vs wave frequency ω/ω_p, where k_D is the inverse of the Debye length. A branch labeled a is a mode of beam space charge wave, and a branch labeled b is a mode of electron plasma wave.
Lower : Growth rate of the branch a vs ω/ω_p.

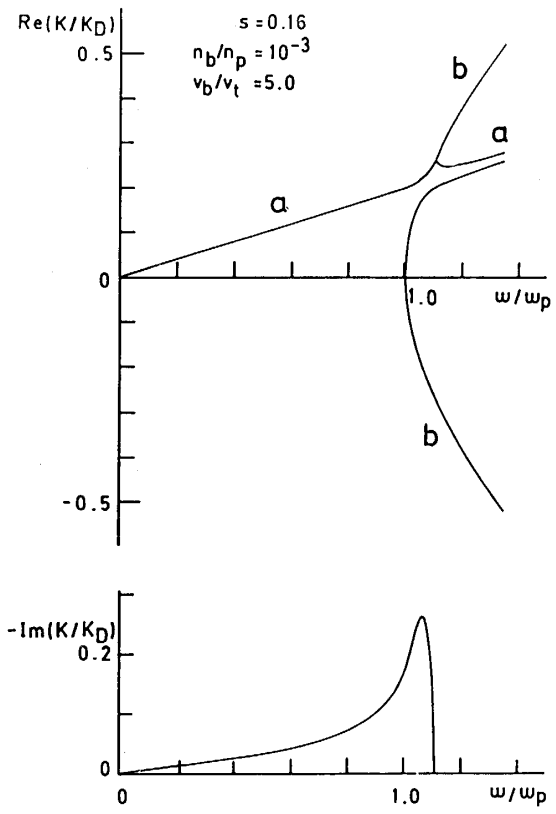

Fig. 2 Numerical solution of the linear dispersion equation in a beam–plasma system (Case II).
Upper : Real part of k/k_D vs ω/ω_p.
Lower : Growth rate of the branch a vs ω/ω_p.

labeled b is a mode of electron plasma wave. Beam–plasma instability can excite the mode of beam space charge wave whose growth rate is also shown in the figures. Generally, the frequency of the most unstable wave ω_0 is determined from the point where the branch of the electron plasma wave and that of the beam space charge wave intersect. Apparently, the half–width of the growth rate in Fig. 2 is larger than one in Fig. 1.

3.2 Wave power enhancement and corresponding behaviors of beam electrons (Case I)

Figure 3 shows typical examples of the wave evolutions in the absence of E_{dc} (a), and in the presence of E_{dc} (b). The behavior of the total power E^2 and that of predominant modes are presented. In Fig. (a), E^2 grows exponentially, saturates and then executes three amplitude oscillations.[11] This amplitude oscillation is caused by the energy ex-

change between the wave and the trapped particles in the potential well of the wave. Up to the third peak of E^2, the most unstable wave with frequency ω_0(labeled 0) dominates both the linear and the nonlinear evolution of the system. However, in the nonlinear stage, the neighboring wave (labeled 1) whose frequency is larger than ω_0 is excited.

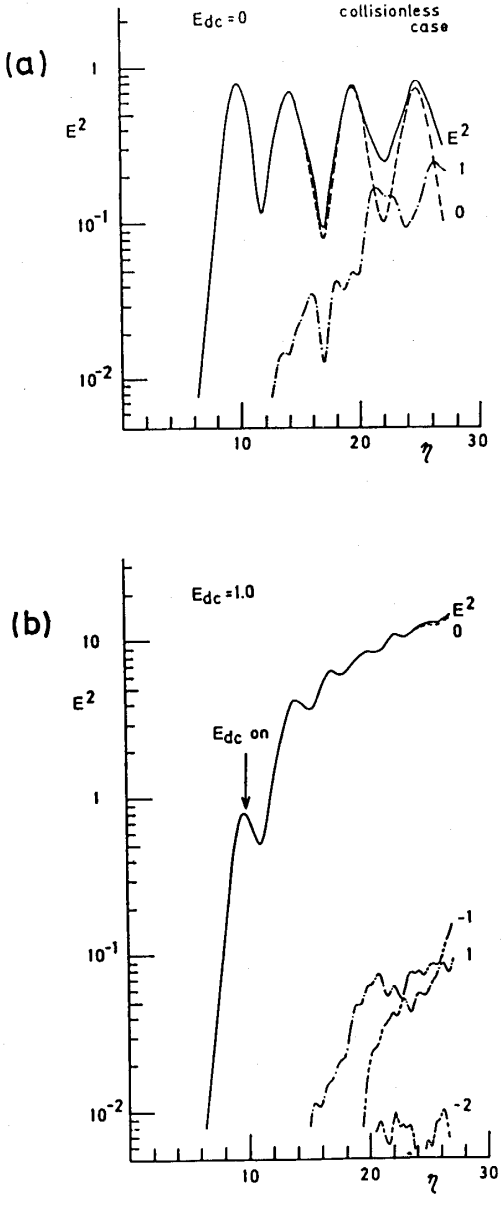

Fig. 3 Spatial evolutions of the total wave power E^2 and the power in the spectral components in the absence of E_{dc} (a), and in the presence of E_{dc} (b). These are computed with 600 beam electrons by using 11 modes system, where $\Delta\omega/\omega_0 = 0.02$. Plasma parameters are $n_b/n_p = 3.1\times10^{-4}$, $v_b/v_t = 9$ and $\nu/\omega_0 = 0$ (Case I).

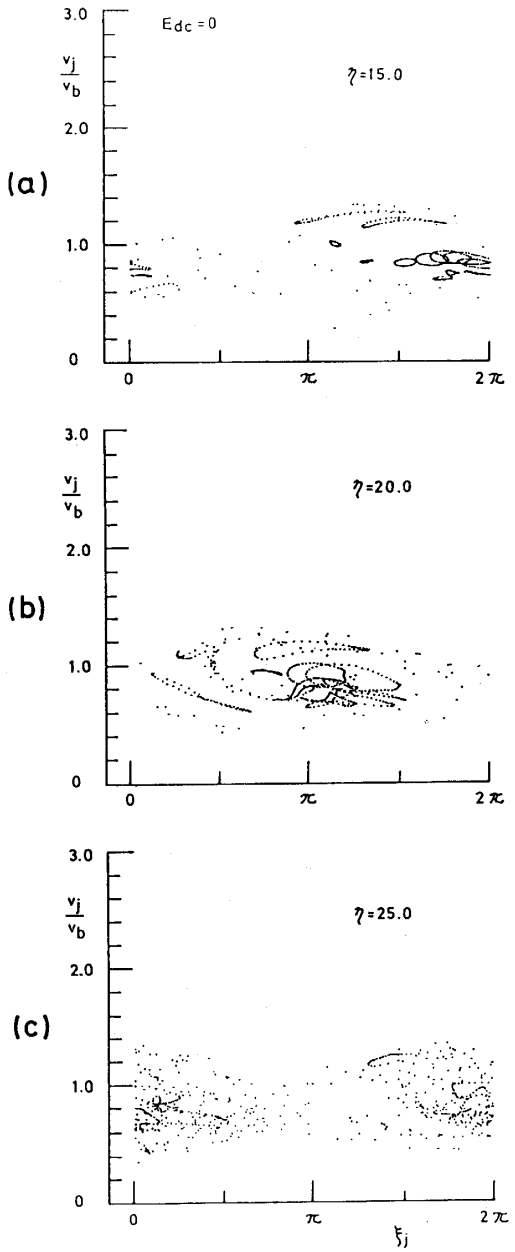

Fig. 4 Phase–space dynamics at three positions corresponding to the wave evolutions in Fig. 3 (a). As $\omega_0/\Delta\omega = 50$, we need to follow the particles whose initial phases are in the interval, $0 \leq \xi_j(0) \leq 100\pi$. In this figure, however, instantaneous particle phase $\xi_j(\eta)$ is transformed in the interval, $0 \leq \xi_j(\eta) \leq 2\pi$.

Then, after the third peak, regular amplitude oscillations of E^2 are deformed due to the effects of the neighboring wave. In the presence of E_{dc}, the saturation amplitude increases and E^2 grows secularly. Although the wave with ω_0 dominates the evolution of the system, the neighboring waves (labeled -1 and -2) whose frequencies are lower than ω_0 are excited in the nonlinear stage.

The simple picture of the E_{dc} effect is as follows.[4,5] When the particles are trapped in the well of the wave, the response of the particles to E_{dc} cannot be a uniform acceleration because they are constrained to move at the phase velocity of the wave. Namely, the particle momentum cannot change in response to E_{dc}. Hence, the wave power can be increased.

Figures 4 and 5 show the phase–space plots at three points (η = 15, 20 and 25), corresponding to the wave evolutions in the absence and presence of E_{dc}, respectively.

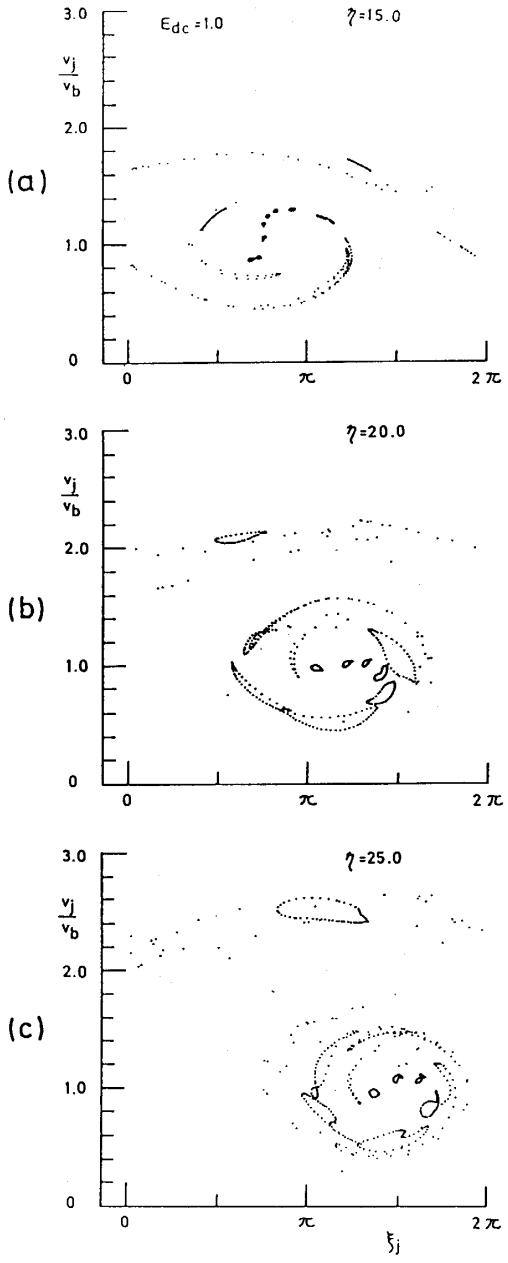

Fig. 5 Phase–space dynamics corresponding to the wave evolutions in Fig. 3 (b). Conditions for plotting beam electrons are the same as ones in Fig. 4.

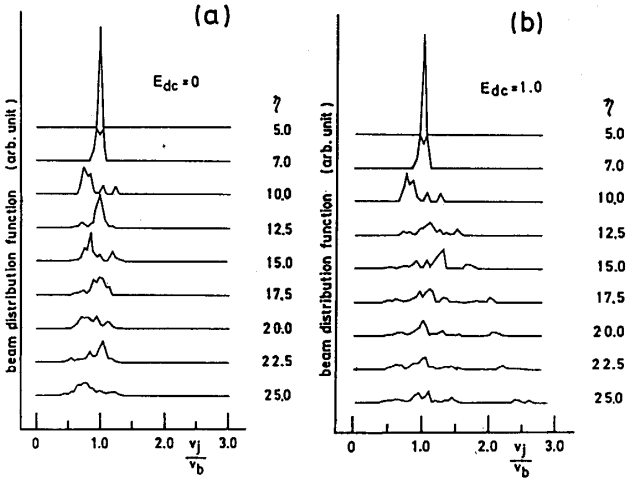

Fig.6 The phase averaged velocity distributions vs v/v_b in the absence of E_{dc} (a), and in the presence of E_{dc}(b).

When E_{dc} is applied, the beam electrons split into two groups : The one with high velocity has runaway electrons and other with low velocity has trapped electrons. The average velocity of runaway electrons increases secularly. For reference, the phase averaged velocity distributions at various positions are also shown in Fig. 6.

When E_{dc} is strong enough to detrap the particles, the particles accelerate and the

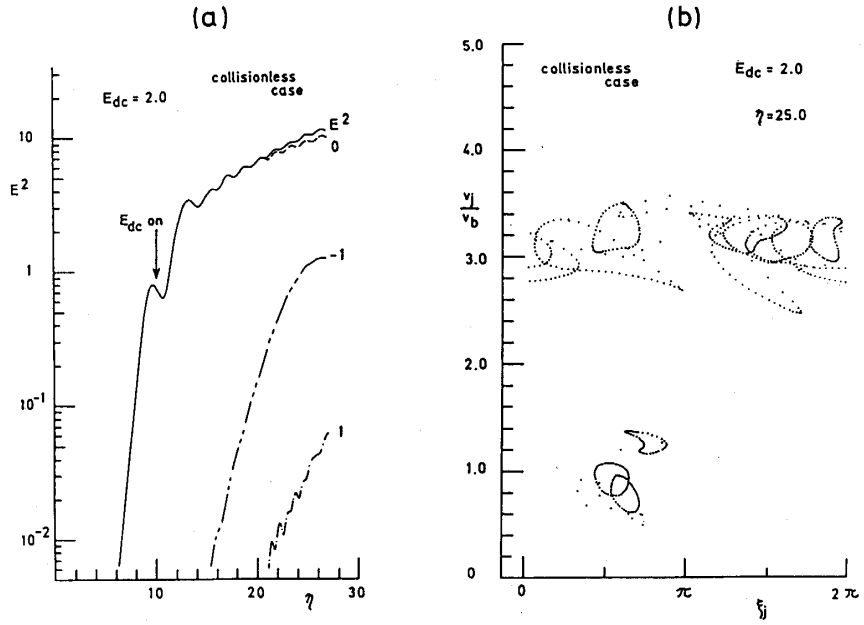

Fig. 7 Wave power evolutions for $E_{dc} = 2$(a), and corresponding phase–space dynamics at $\eta = 25$ (b). Other numerical conditions are the same as ones in Fig. 3.

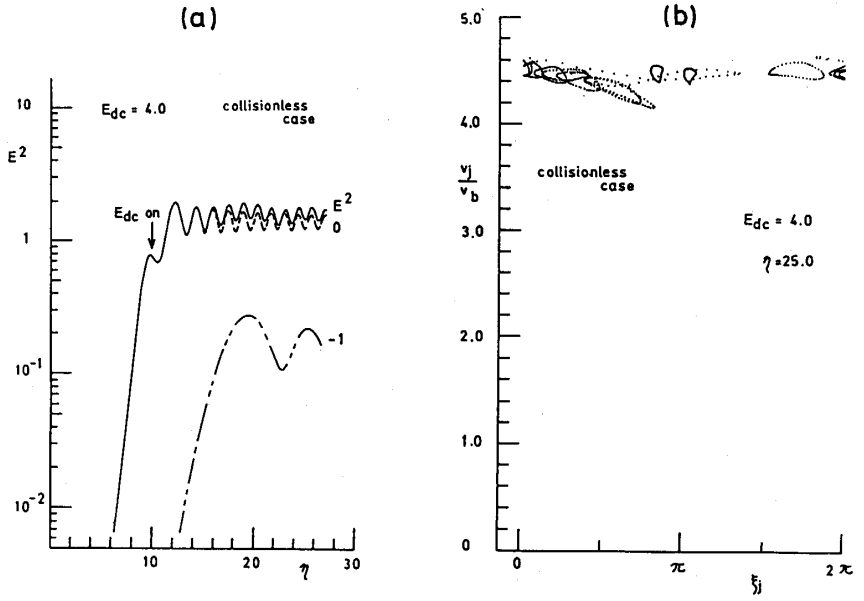

Fig. 8 Wave power evolutions for $E_{dc} = 4$ (a), and corresponding phase–space dynamics at $\eta = 25$ (b). Other numerical conditions are the same as ones in Fig. 3.

wave enhancement does not occur. Qualitatively, the E_{dc} effect is classified into two cases, i. e. production of runaway beams and wave enhancement, based on a criterion $E_{dc} > E_s$ or vice versa. Here, E_s is the saturation amplitude for $E_{dc} = 0$. Of course the system can be satisfied by having both states simultaneously, i. e. some of the beam electrons run away while others remanin clamped as shown in Fig. 5.

Figures 7 and 8 show the examples of the wave evolutions for the strong E_{dc}. With increasing E_{dc}, the ratio of runaway electrons to total electrons increases and wave en-

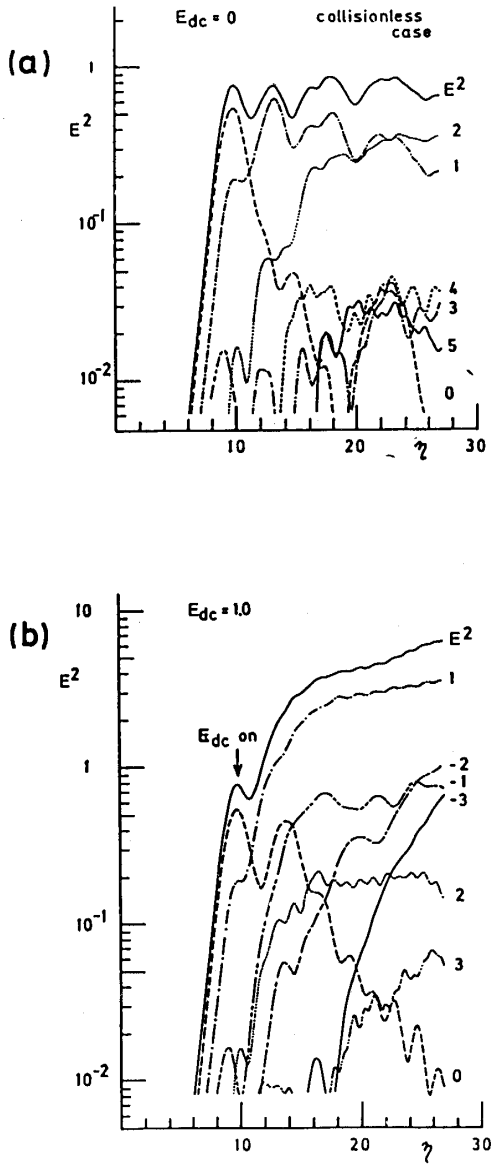

Fig. 9 Wave power evolutions in the absence of E_{dc} (a), and in the presence of E_{dc} (b). Plasma parameters are $n_b/n_p = 10^{-3}$, $v_b/v_t = 5$ and $\nu/\omega_0 = 0$ (Case II). Other numerical conditions are the same as ones in Fig. 3.

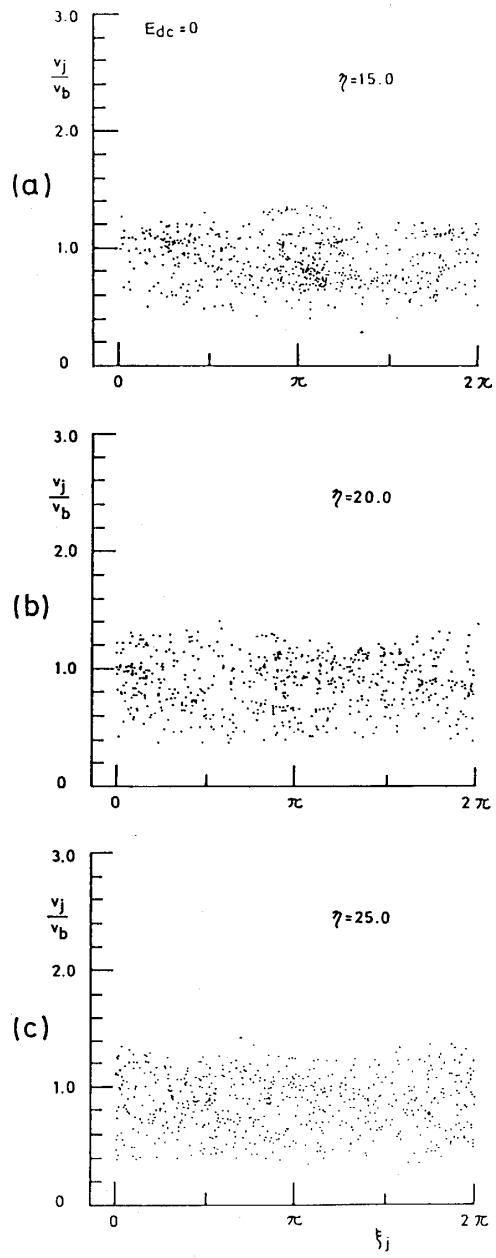

Fig. 10 Phase–space dynamics corresponding to the wave evolutions in Fig. 9(a).

hancement caused by E_{dc} decreases. When $E_{dc} = 4$, all electrons are detrapped and accelerated secularly.

3.3 Wave power enhancement and corresponding behaviors of beam electrons (Case II)

Figure 9 shows the examples of the spatial evolutions of the wave power. According to Fig. (a), the most unstable wave with ω_0 no longer dominates the evolution of the system during a linear growth region. Then, in the nonlinear stage, the regular amplitude osillation of the total wave power E^2 is destroyed due to many wave effects.[10,11] Although with applying E_{dc} the wave power E^2 is observed to grow secularly, the effect

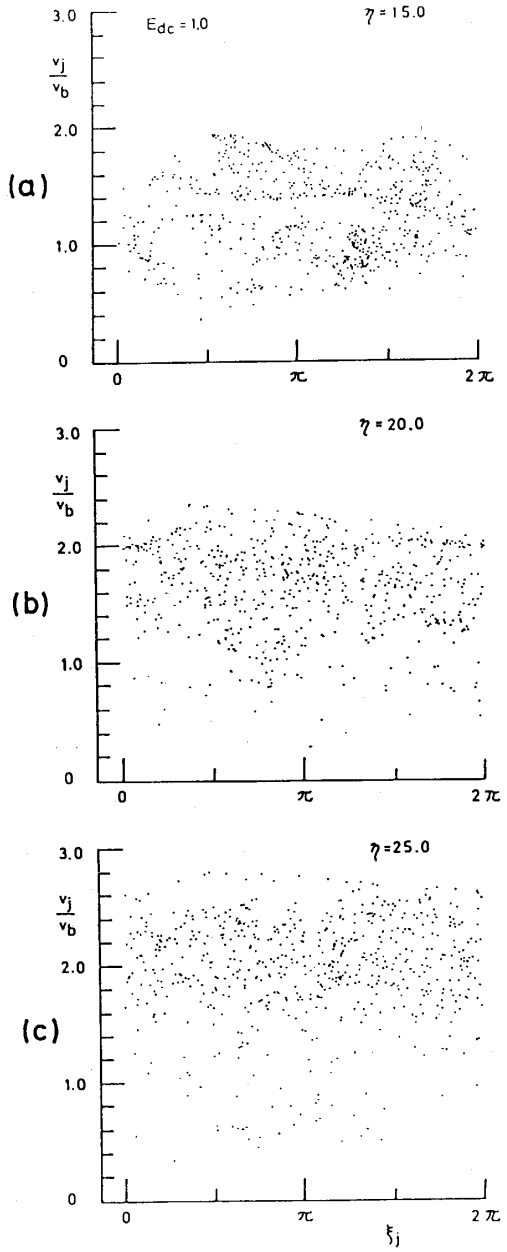

Fig. 11 Phase-space dynamics corresponding to the wave evolutions in Fig. 9(b).

of E_{dc} on wave enhancement is not so remarkable as one for Case I (see Fig. 3).

The behaviors of neighboring waves, however, have the same tendencies as ones have in Case I. The waves whose frequencies are higher than ω_0 grow easily in the absence of E_{dc}. On the other hand, in the presence of E_{dc} the waves whose frequencies are lower than ω_0 become predominant.

These results are well explained qualitatively by the characteristics of the linear dispersion relation (see Figs. 1 and 2) . With the increase in wave amplitude, in the absence of E_{dc}, ω_0 is varied from the initial point to the higher side due to the slowing down of the injected beams. Because ω_0 is determined from the point where the branch a and the branch b intersect, and the slope of the branch a is proportional to the inverse of the average beam velocity. Sideband waves with ω (higher than ω_0) become more resonant to the slowed beam–plasma system. When trapped electrons are accelerated, however, the average beam velocity increases. Then, ω_0 is varied from the initial point to the lower side and sideband waves with ω (lower than ω_0) become more resonant to the system.

Figures 10 and 11 show the phase–space plots corresponding to the wave evolutions in Fig. 9. Because of the neighboring waves growth, in Fig. 10, the bunching of the beam electrons is deformed and the beam electrons are smeared out in the early nonlinear stage. Therefore, in Fig. 11, the response of the beam electrons to E_{dc} seems to be a uniform acceleration because the beam electrons cannot be constrained to move at the phase velocity of the most predominant wave. As the wave–particle resonance is detuned by increasing runaway electrons, wave power enhancement in Fig. 9 is not so remarkable.

Figure 12 shows the phase averaged velocity distributions corresponding to wave evolutions in Fig. 9.

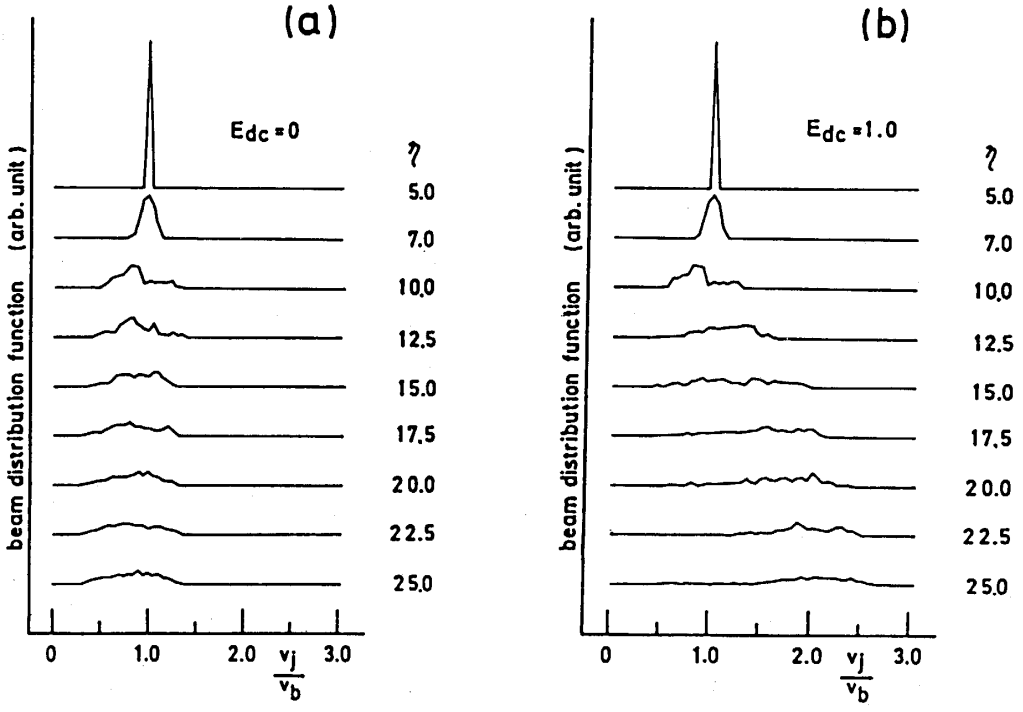

Fig. 12 The phase averaged velocity distributions vs v/v_b.

3.4 Effects of weak collisions on wave enhancement

Previously, we showed that collisional effects play an important role in the nonlinear wave–particle interaction even if collisions are too weak to change the linear stage.[12)]

Figure 13 illustrates the evolution of the wave in the presence of weak collisions (Case I) . Up to the wave saturation ($\eta = 10$), in Fig. (a), weak collisions cannot change the behavior of the system in comparison with that of the collisionless system (see Fig. 3). After this point, however, the most unstable wave damps to the first minimum strong-

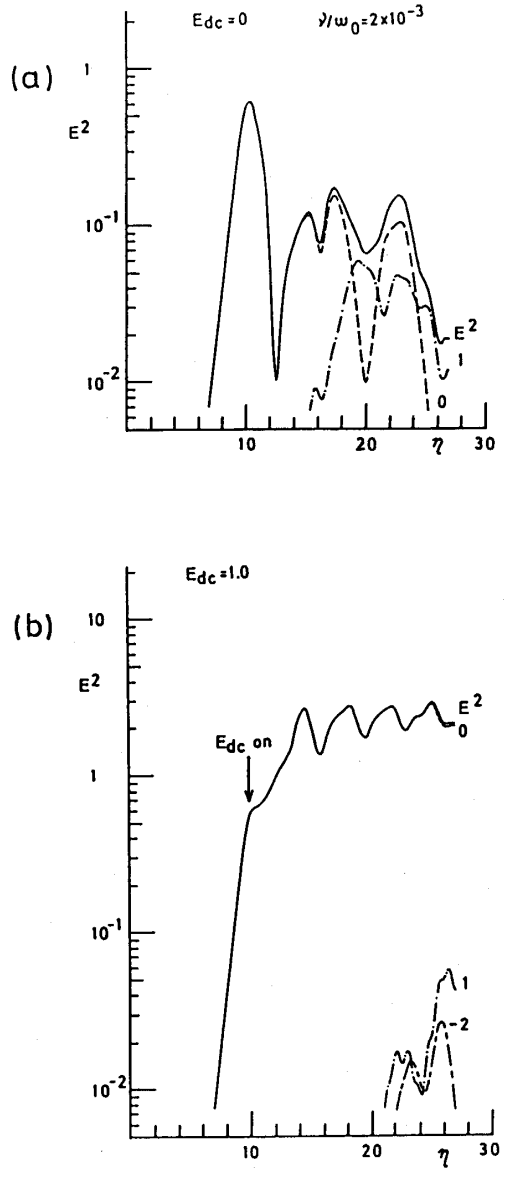

Fig. 13 Wave power evolutions in the presence of weak collisions for Case I, where $\nu / \omega_0 = 2\text{x}10^{-3}$. Other numerical conditions are the same as ones in Fig. 3.

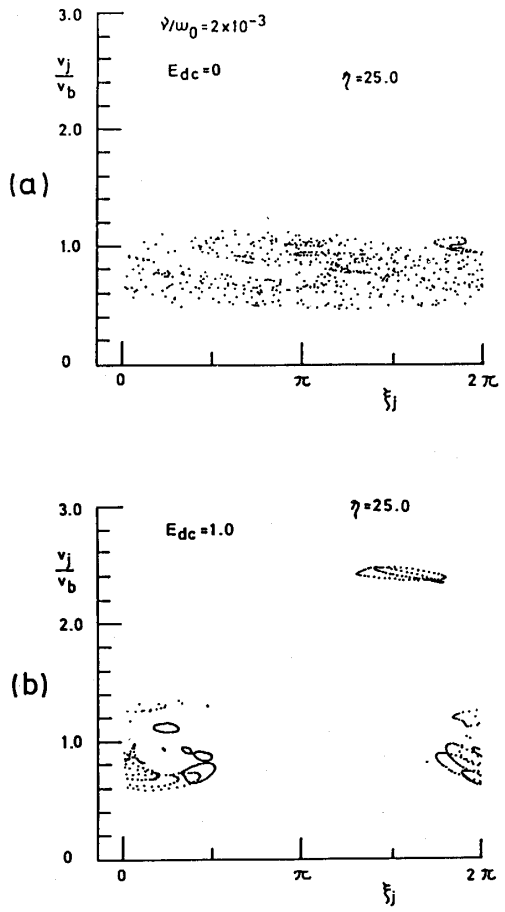

Fig. 14 Phase–space dynamics corresponding to the wave evolutions in Fig. 13.

ly and fails to regrow to the level of the first maximum. The amplitude oscillations of E^2 is changed drastically and destroyed.[12] From Fig. (b), wave enhancemet is strongly limited to a lower level by collisional effects. Corresponding phase–space plots are shown in Fig. 14.

Figures 15 and 16 show the evolutions and the corresponding phase–space plots for Case II, respectively.

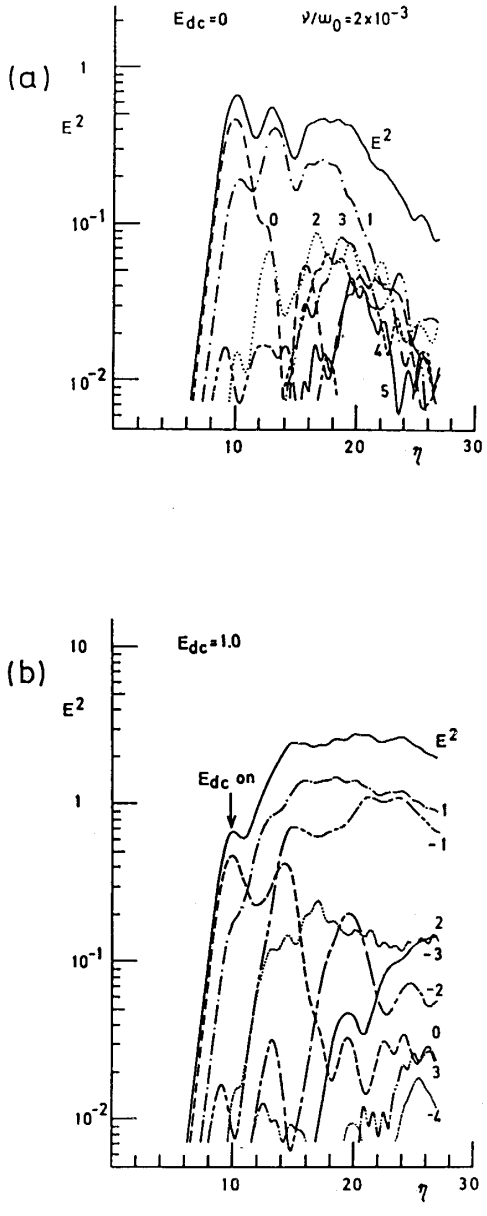

Fig. 15 Wave power evolutions in the presence of weak collisions for Case II, where $\nu / \omega_0 = 2\times10^{-3}$. Other numerical conditions are the same as ones in Fig. 9.

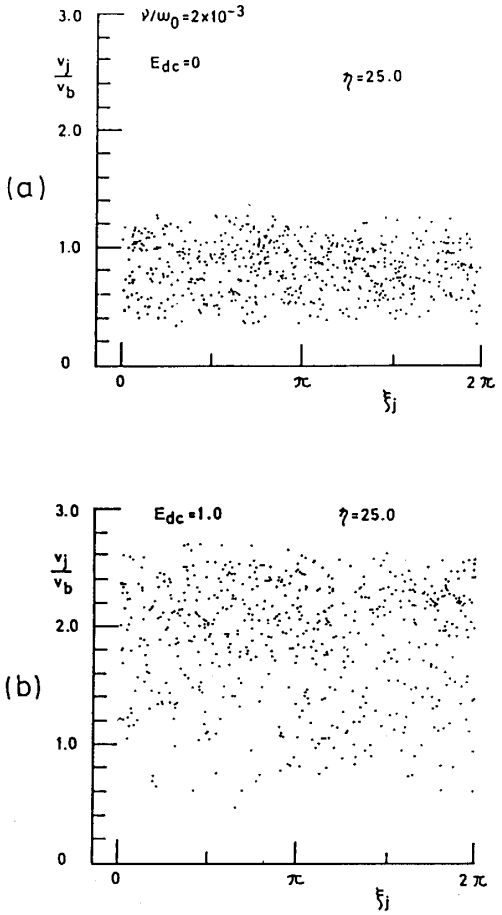

Fig. 16 Phase–space dynamics correponding to the wave evolutions in Fig. 15.

4. Conclusion

The role of E_{dc} on the nonlinear wave–particle interaction in a small cold beam–plasma system is investigated by using the model of many waves. The model includes eleven modes and weak collisional effects in the plasma.

Particularly, the control of wave power caused by E_{dc} has been studied. In the absence of collisions, the beam momentum can be clamped while the wave power increases secularly for the moderate E_{dc}. However, the wave enhancement depends on the growth of neighboring waves. The effect of E_{dc} is most significant when the system excites almost the monochromatic wave. Besides these, weak collisions ($\nu / \omega_0 \sim 10^{-3}$) play an important role in limiting the wave power enhancement.

Acknowledgments

We wish to thank M. Yasutake for assistance with programming and calculations. Numerical computations were carried out at the Yamaguchi University Computer Center.

References

1) Drummond, W. E., Malmberg, J. H., O'Neil, T. M. and Thompson, J. R., Phys. Fluids, **13**, 2422 (1970).
2) O'Neil, T. M., Winfrey, J. H. and Malmberg, J. H., Phys. Fluids, **14**, 1204 (1971).
3) Gentle, K. W. and Lohr, J., Phys. Fluids, **16**, 1464 (1973).
4) Morales, G. J., Phys. Fluids, **23**, 2472 (1980).
5) Tsunoda, S. I. and Malmberg, J. H., Phys. Fluids, **27**, 2557 (1984).
6) Lin, A. T., Phys. Rev. Lett., **46**, 1515 (1981).
7) Fukumasa, O. and Saeki, S., Memoirs of the Faculty of Engineering, Yamaguchi University, **35**, 171 (1984) (in Japanese).
8) Fukumasa, O. and Saeki, S., Phys. Fluids, **28**, 1754 (1985).
9) Winfrey, J. H. and Dunlop, M. L., Plasma Phys., **19**, 901 (1977).
10) Fukumasa, O., Abe, H. and Itatani, R., Research Report of Institute of Plasma Physics, Nagoya University, IPPJ–407 (1979).
11) Fukumasa, O., Abe, H. and Itatani, R., Plasma Phys., **24**, 843 (1982).
12) Fukumasa, O., Abe, H. and Itatani, R., Phys. Rev. Lett., **40**, 393 (1978).